Available online at www.sciencedirect.com
ScienceDirect
Trans. Nonferrous Met. Soc. China 32(2022) 3810−3821
Transactions of Nonferrous Metals Society of China
www.tnmsc.cn

An environmentally benign and sustainable process for carbon recovery and efficient defluorination of spent carbon cathode

Yi-fan LI[1*], Hao CHENG[1*], Pei-yu GONG[1], Kai YANG[2], Zhong-liang TIAN[1], Yan-qing LAI[1]

1. School of Metallurgy and Environment, Central South University, Changsha 410083, China;
2. School of Metallurgical Engineering, Xi'an University of Architecture and Technology, Xi'an 710055, China

Received 19 January 2022; accepted 15 August 2022

Abstract: A systematic and green low-temperature sulfation roasting−water leaching strategy was put forward to achieve a very high fluorine removal rate of 97.82% for spent carbon cathode (SCC), which was believed as a hazardous solid waste. And the carbon could be recycled with a purity of 90.29 wt.% in the flaky microstructure. Thermodynamic analysis and the results of SEM, XRD and EDS indicate that most of the fluoride could convert into water-soluble sulfate at low temperature. And the highest fluorine removal rate could be obtained when <0.15 mm SCC particles were mixed with sulfuric acid at a liquid-to-solid ratio of 1:1, and then roasted at 300 °C for 0.5 h. The sulfate was removed to purify the carbon via water-leaching process. Avrami exponents and corresponding activation energy for the roasting and leaching process demonstrated that both processes are controlled by diffusion.
Key words: spent carbon cathode; defluorination; sulfation roasting; water-leaching; kinetics analysis

1 Introduction

The carbon cathode of the aluminum electrolysis cell would be broken and cracked due to the erosion of electrolyte, sodium, molten aluminum and series of fluorides in Hall−Héroult process [1,2]. It is necessary to overhaul and replace them to maintain the normal production every 3−8 years [3,4]. And more than 650 thousand tons of the spent carbon cathode (SCC) were discharged with global primary aluminum production of 65.33 million tons in 2020 [5,6]. Meanwhile, SCC is the main hazardous solid wastes generated from the primary aluminum electrolysis process due to the presence of soluble fluoride and cyanide [7]. It will bring a series of hazards to human activities and ecological environment if not handled properly [8]. The available carbonaceous materials and fluorides also display the high recovery potential and economic benefits [9]. Thus, it is highly desirable to achieve the harmless treatment and effective resource reuse of SCC.

Researchers have explored a variety of technologies to realize the detoxification of SCC since the late 1970s [10]. It is widely adopted to carry out the chemical leaching, molten salt roasting, high temperature hydrolysis, flotation, vacuum distillation and coprocessing with other solid wastes to disposal SCC [11−16]. However, a great deal of carbonaceous materials would be consumed and fluorine-containing flue gas could corrode equipment under high temperature conditions (above 600 °C) [10]. And high consumption of solvents and a large amount of fluoride-containing wastewater increase the cost of the leaching methods [17]. Recycled carbon materials are also mixed with more fluorides, limiting the further application of the product [18]. Therefore, a simple process without secondary

Yi-fan LI and Hao CHENG contributed equally to this work
Corresponding author: Zhong-liang TIAN, E-mail: tianzhongliang@csu.edu.cn; Yan-qing LAI, E-mail: laiyanqing@csu.edu.cn
DOI: 10.1016/S1003-6326(22)66060-6
1003-6326/© 2022 The Nonferrous Metals Society of China. Published by Elsevier Ltd & Science Press

pollution for efficient separation of carbonaceous materials and fluorides is imperative for the sustainable and economic development of aluminum metallurgy industry.

The effective conversion of fluorides is the key to realize the harmless treatment of SCC. Fluorite−sulfuric acid process is widely applied to producing the hydrogen fluoride (HF) at a low temperature, which is the vital industrial raw material [19]. PAULINO et al [20] used cryolite as a raw material to react with sulfuric acid and eventually converted more than 96% of fluorine to hydrogen fluoride. DYACHENKO et al [21,22] proposed a sulfation roasting process to prepare hydrogen fluoride using fluorinated waste from aluminum electrolysis with the fluorine conversion rate of 97%, and reduced production cost of hydrogen fluoride by 20%. MATHIESSEN et al [23] used sulfuric acid to acidify fluoride-containing wastewater with a vigorous argon flow into the solution, achieving that [^{18}F] fluoride was recovered as [^{18}F] HF gas with the recovery rate of 82%. These studies indicated that the fluorine in the fluoride could react with sulfuric acid to generate hydrogen fluoride gas at a relatively lower temperature.

In this work, the systematic low-temperature sulfation roasting−water leaching process is proposed to achieve the efficient separation of carbonaceous materials and fluorides, which realizes efficient cleaning treatment of SCC. And fluoride is finally transformed into the hydrogen fluoride gas and sulfate, which avoids the generation of high temperature fluorine-containing flue gas and fluoride-containing wastewater. Compared to the research reported, a very high fluorine removal rate of 97.82% and a high flaky carbon purity of 90.29 wt.% could be obtained for SCC. The experimental design and analysis of the kinetic characteristics were combined to reveal the regulation mechanism of phase transformation during the process of sulfation roasting defluorination. And the whole process is carried out at a low temperature compared with the existing defluorination process. Therefore, the proposed method with environment benignity, economic feasibility and appealing efficiency provides an alternative way to achieve comprehensive harmless treatment and recovery of SCC, which is of great noteworthiness to the green development of the aluminum industry chain.

2 Experimental

2.1 Materials and reagents

SCC was gathered from an aluminum electrolysis plant (Sichuan, China) in this study. Sodium hydroxide (NaOH, analytical grade) and concentrated sulfuric acid (H_2SO_4, 98%) were acquired from Sinopharm Chemical Reagent Co., Ltd. And aluminum hydroxide ($Al(OH)_3$) solution (1 mol/L) was compounded with homemade deionized water, which was also purchased from Sinopharm Chemical Reagent Co., Ltd. (China).

2.2 Experimental procedure

The process flow sheet for the disposal of SCC by way of low-temperature sulfation roasting and water leaching is exhibited in Fig. 1. SCC was comminuted by a high-efficient crusher and the crushed sample was dehydrated in a blast drying stove at (105±1) °C for 4 h. Then, 4 g sample powder was mixed with concentrated sulfuric acid in a fume hood for 10 min. And the medley was located in a pipe furnace and heated up to target temperature with a ramping rate of 5 °C/min. The hydrogen fluorine gas produced during roasting process was absorbed by $Al(OH)_3$ solution and exhausted to atmosphere. And 5 g of finely ground roasted residue was leached with deionized water in a 200 mL glass beaker at target temperature. Carbonaceous materials obtained by vacuum filtration was dried in a blast drying oven at 110 °C.

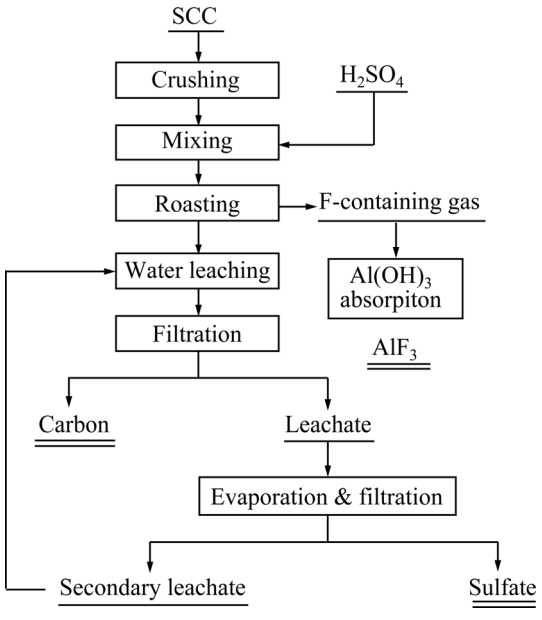

Fig. 1 Flowchart for series manipulation process of SCC

The leachate containing a large amount of sulfate can be further processed to obtain sulfate.

2.3 Analysis and characterization

The removal rate (X/%) of fluorine of SCC was worked out via the following Eq. (1). Dried carbon materials were burnt up in a muffle oven at 800 °C for 4 h. Then, carbon content (W/wt.%) of materials was reckoned by the subsequent Eq. (2) after leaching procedure [18]:

$$X=[1-w_2m_2/(w_1m_1)]\times100\% \quad (1)$$

$$W=(1-m_4/m_3)\times100\% \quad (2)$$

where w_1 is the fluorine content of the SCC, g/kg; m_1 means the initial mass of the SCC, g; w_2 represents the fluorine amount of roasted residue, g/kg; m_2 implies the mass of roasted remnant, g; m_3 is the primary mass of leaching residue, g; m_4 is mass of leaching residue after incinerating, g.

The consistence of fluoride ions was measured by using the ion meter (PXSJ−216). X-ray fluorescence spectrometry (XRF, Vario El III) was used to analyze the elemental composition of the specimen. X-ray diffraction (XRD, Rigaku3014) analysis was also adopted to investigate the phase of sample by using Cu K_α radiation (λ=1.54056 Å). Then, the micro morphology of SCC was determined through scanning electron microscope (SEM, JSM−6360LV). Analysis of the surface ingredient of specimen was executed by energy dispersive X-ray spectroscopy (EDX, QENESIS 60S).

3 Results and discussion

3.1 Characteristic of SCC

The element and proximate analysis results of SCC are displayed in Table 1 and Fig. 2(a), respectively. And the XRD pattern is depicted in Fig. 2(b). It could be found that fixed carbon (FC_{ad}, 63.04 wt.%) and ash (A_{ad}, 34.13 wt.%) are the main phases. There is also some water (M_{ad}, 0.95 wt.%) and volatile matter (V_{ad}, 1.88 wt.%) in the SCC. In order to further study the impurity composition in SCC, the sample was oxidized and roasted at 850 °C to remove carbonaceous materials and ash. The results are shown in Fig. 2(c). NaF (PDF #36-1455), CaF_2 (PDF #77-2093), Al_2SiO_5 (PDF #11-0046), Na_3AlF_6 (PDF #18-1214) and Al_2O_3 (PDF #50-0741) could be confirmed in the XRD pattern. The carbon (dark matter) and electrolyte (gray matter) are mechanically mixed together in the form of adhesion (Fig. 3). It could be known that the concentration of fluorine is 6169 mg/L by the analysis of soluble fluorine content of SCC.

Table 1 Element analysis result of SCC (wt.%)

C	Na	F	Al	Ca	O
63.04	10.32	9.77	6.30	3.89	2.90
Fe	K	Si	S	Others	
1.43	1.02	0.42	0.30	0.61	

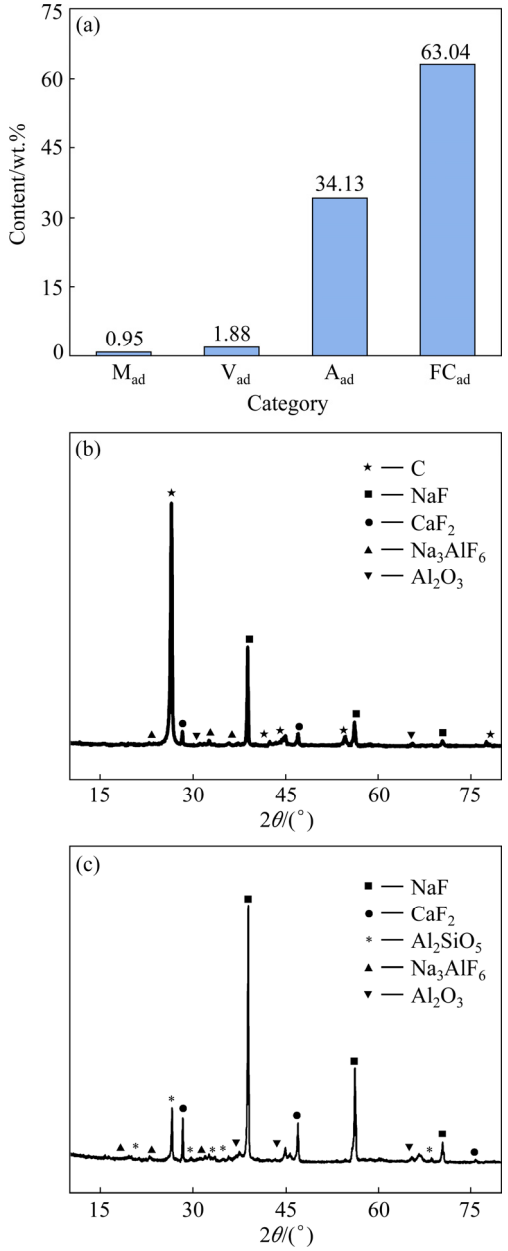

Fig. 2 Proximate analysis result of SCC (a), XRD patterns for SCC (b) and impurities (c)

3.2 Thermodynamic analysis

The main reactions between impurities and sulfuric acid occurring in the roasting process are listed in Table 2. Furthermore, the relationship between standard Gibbs free energy change of reaction ($\Delta_r G_T^{\Theta}$) and temperature are illustrated in Figs. 4(a, b). The thermodynamic data of the reaction were referenced from the HSC Chemistry 9.0 software. It was shown that values of $\Delta_r G_T^{\Theta}$ were more negative when NaF, Ca_2F, Na_3AlF_6, Al_2O_3, and Al_2SiO_5 reacted with sulfuric acid at 100−300 °C, indicating that the reactions could proceed spontaneously in this range of temperature [24]. Therefore, the roasting process could be carried out at a comparatively low temperature. The fluorine of SCC was converted to sulfate and HF during roasting process, which could be recycled by further processing, as illustrated in Fig. S1.

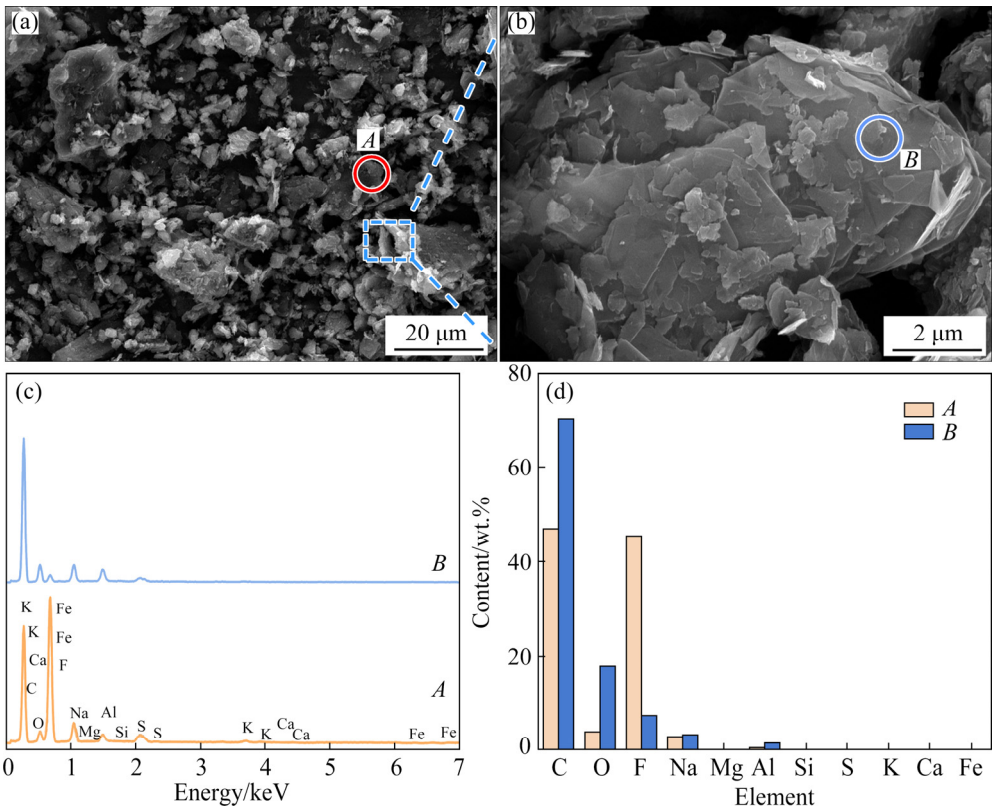

Fig. 3 SEM images (a, b) and local sites EDS results (c, d) of SCC

Table 2 Equilibrium reactions in sulfation roasting process

Reaction	$\Delta_r G_T^{\Theta}-T$ equation	No.
$NaF+H_2SO_4=NaHSO_4+HF(g)$	$\Delta_r G_T^{\Theta}=-10.42-0.08T$	(3)
$NaHSO_4+NaF=Na_2SO_4+HF(g)$	$\Delta_r G_T^{\Theta}=39.38-0.16\ T$	(4)
$CaF_2+H_2SO_4=CaSO_4+2HF(g)$	$\Delta_r G_T^{\Theta}=56.11-0.23T$	(5)
$Na_3AlF_6+3H_2SO_4=3NaHSO_4+AlF_3+3HF(g)$	$\Delta_r G_T^{\Theta}=46.97-0.22T$	(6)
$2AlF_3+3H_2SO_4=Al_2(SO_4)_3+6HF(g)$	$\Delta_r G_T^{\Theta}=392.50-0.68T$	(7)
$Al_2O_3+3H_2SO_4=Al_2(SO_4)_3+3H_2O(g)$	$\Delta_r G_T^{\Theta}=-43.24-0.28T$	(8)
$Al_2SiO_5+3H_2SO_4=Al_2(SO_4)_3+3H_2O(g)+SiO_2$	$\Delta_r G_T^{\Theta}=-35.04-0.29T$	(9)
$C+H_2SO_4=CO(g)+H_2O(g)+SO_2(g)$	$\Delta_r G_T^{\Theta}=164.83-0.47T$	(10)
$C+2H_2SO_4=CO_2(g)+2H_2O(g)+2SO_2(g)$	$\Delta_r G_T^{\Theta}=157.24-0.77T$	(11)
$H_2SO_4=H_2O(g)+SO_3(g)$	$\Delta_r G_T^{\Theta}=176.42-0.29T$	(12)

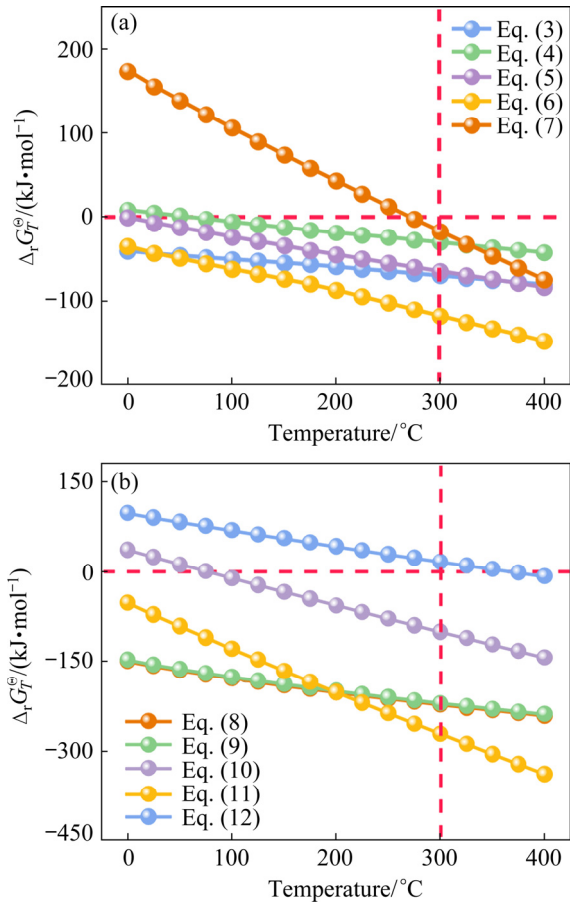

Fig. 4 Relationship between $\Delta_r G_T^{\ominus}$ and temperature of fluoride (a) and other compounds (b)

3.3 Sulfation roasting condition optimization

A single-variable trial was performed to select the sulfation roasting condition and the effects of particle size of SCC, liquid to solid ratio, roasting time and temperature on fluorine removal rate are exhibited in Fig. 5. The content of fluorine in SCC showed a trend of decreasing and then increasing with the decrease of particle size, as illustrated in Fig. 5(a). And the content of fluorine decreased from 106.56 to 97.10 g/kg when the particle size was reduced from 0.60−1.18 to 0.15−0.30 mm. The result was attributed to the fact that the carbon and electrolyte were wrapped together and were difficult to separate, resulting in a higher fluorine content when the particle size was larger. And it gradually increased to 117.81 g/kg with a greater decline in the grain size to <75 μm [25,26]. The fluoride electrolyte showed poor ductility and higher brittleness, which made it easier to break into fine particles and enriched at 75 μm. The removal rate of fluorine increased from 89.12% to 96.86% with the decrease of particle size from 0.60−1.18 to <0.15 mm. And the fluorine removal rate was 97.79% when particle size was further decreased to <75 μm, which may be influenced by the fluorine content instead of particle size. Therefore, the particle size of <0.15 mm was chosen.

Removal rate of fluorine showed an increase trend as the temperature rose (Fig. 5(b)). The viscosity of sulfuric acid decreased with the ascent of the roasting temperature. This was conducive to the improvement of mass transport process and the penetration ability to the inside of the carbon materials to react with the fluoride electrolyte [27]. However, the decomposition and volatilization of the sulfuric acid would also deteriorate the defluorination efficiency. Therefore, 300 °C was the favorable roasting temperature for the reaction of sulfuric acid and fluoride, at which the removal rate of fluorine is 96.13%. Figure 5(c) indicated that the removal rate of fluorine increased slightly in the roasting time scope from 0.5 to 3.0 h. The corresponding removal rate increased by 1.20% from 95.66% to 96.86%. Consequently, the optimal roasting time is 3.0 h. The removal rate of fluorine conveyed a trend of rapid increase (96.86%) and then stabilization following the ascent of liquid-to-solid ratio to 1:1 (Fig. 5(d)). The increase of sulfuric acid improved the fluidity of mixture and promoted the mass transfer by diffusion, contributing to the favorable development of the chemical reaction [28]. And it also implied that there was only an improvement of 1.09% when the liquid-solid ratio continued to increase to 1.5:1. Consequently, the optimum liquid-to-solid ratio was 1:1.

To investigate the influence of different roasting process parameters on the fluorine removal rate in SCC and to determine the optimal process parameters, the effects of experimental factors (particle size (A), roasting time (B), roasting temperature (C) and liquid-to-solid ratio (D)) were probed by an orthogonal experiments design. And factors and specific ranges of parameters in "4-factor and 3-level" $L_9(3^4)$ design are listed in Tables S1 and S2. The parameters K_{ij} (arithmetic means of k_{ij}) and R_j were calculated, and the results are depicted in Fig. 5(e). R_j represents the extremum between the maximal and minimal values of K_{ij} corresponding to each factor. And the larger the value of R_j, the greater the influence of the factor [29]. It could be concluded that the order of the values was as follows: $R_D > R_C > R_B > R_A$.

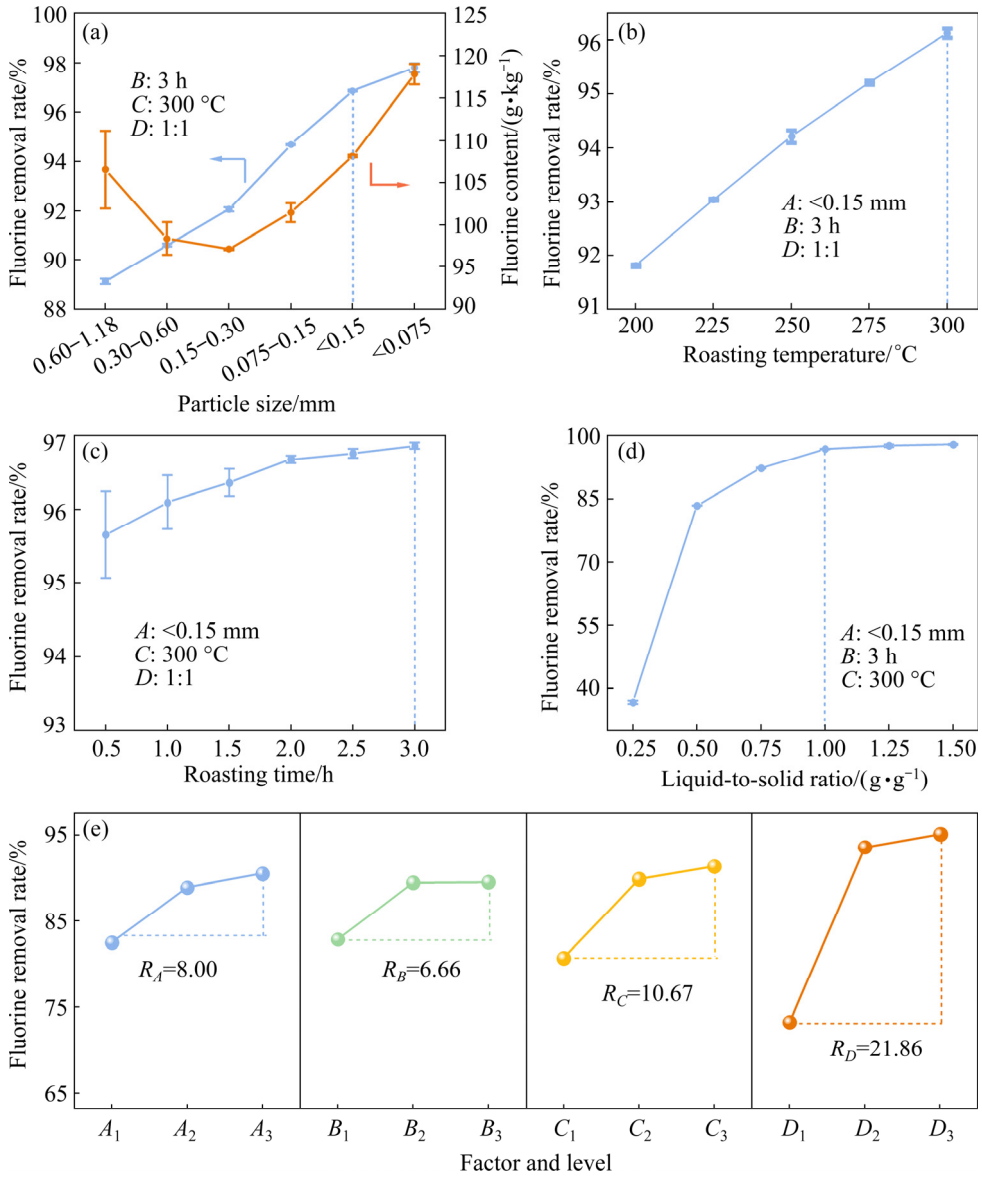

Fig. 5 Effects of process parameters on fluorine removal rate: (a) Particle size; (b) Roasting temperature; (c) Roasting time; (d) Liquid-to-solid ratio; (e) K_{ij} and R_j values of different factors at different levels

Therefore, the liquid-solid ratio has the most dominate influence on the removal rate of fluorine during the roasting process, followed by the temperature, roasting time and particle size. And the best combination for factors was $A_3B_3C_3D_3$, which yielded the fluorine removal rate of 97.82%, higher than all the designed orthogonal experiments. Considering the influence level of each factor, the production cost and the energy consumption, the optimal parameters was determined as particle size of <0.15 mm, roasting time of 0.5 h, roasting temperature of 300 °C and liquid-solid ratio of 1:1.

3.4 Defluorination kinetics analysis

The particle size of raw material was distributed widely and the fluorinated compound was irregularly granular with poor sphericity. Therefore, shrinking core model was not applicable to the defluorination kinetics [20,22]. The fitting data for shrinking core model further demonstrated that the inapplicability of the shrinking core model (Table S3). And Avrami equation (Eq. (13)) was also a good fit for some solid−liquid reaction process, which was used to investigate the crystallization process. It was also used to describe the leaching process since leaching could be regarded as the inverse process of crystallization [30,31]. Additionally, the sulfuric acid is liquid, and the sulfation roasting could also be regarded as a leaching process at a certain

temperature, Hence, Avrami equation could be adopted to describe the roasting process:

$$\ln(-\ln(1-X))=\ln k+n\ln t \quad (13)$$

where k exhibits the reaction rate constant, which keeps associated with the reaction temperature, concentration of solution, reactant particle size, stirring intensity [32]; t is the time, min; n is the Avrami exponent, which is only related to the nature and geometry of the solid grains, and the value of n reflects the mechanism. The beginning reaction rate is near zero while the value of n is over 1. The chemical reaction is the control step for n=1. The reaction is controlled by a mixture of chemical reaction and diffusion when $0.5\leq n<1$. The lixiviate process is a diffusion-control step for n<0.5 [33].

Figure 6(a) depicts the connection between $\ln(-\ln(1-X))$ and $\ln t$ at dissimilar temperatures for roasting process. The linear fitting results are manifested in Table S4. The average of the correlation coefficient at different temperatures was 0.97859, which indicated that the Avrami equation fitted the dynamic model of defluorination process well. And the Avrami exponents n was obtained as 0.05162 (n<0.5), suggesting that the defluorination procedure was restrained by diffusion process. The frequency factor (A') and activation energy (E_a) of the defluorination process were calculated by the Arrhenius equation [34]:

$$\ln k=-E_a/(RT)+\ln A' \quad (14)$$

where R means the molar gas constant and R=8.314 J/(mol·K); T represents the roasting temperature, K.

Moreover, the plot of $\ln k$ versus T^{-1} is shown in Fig. 6(b) for roasting process. The activation energy and frequency factor of the defluorination process were calculated to be 4.89 kJ/mol and 7.42, respectively. The activation energy of the procedure controlled by diffusion is generally around 20 kJ/mol. When the activation energy is greater than 40 kJ/mol, the reaction procedure is predominantly limited by chemical reactions [35]. Therefore, the defluorination procedure was restrained by diffusion, which was in agreement with the result obtained based on n<0.5. And the kinetic equation of the low temperature sulfation roasting is

$$-\ln(1-X)=7.42\exp[-4891/(RT)]t^{0.05162} \quad (15)$$

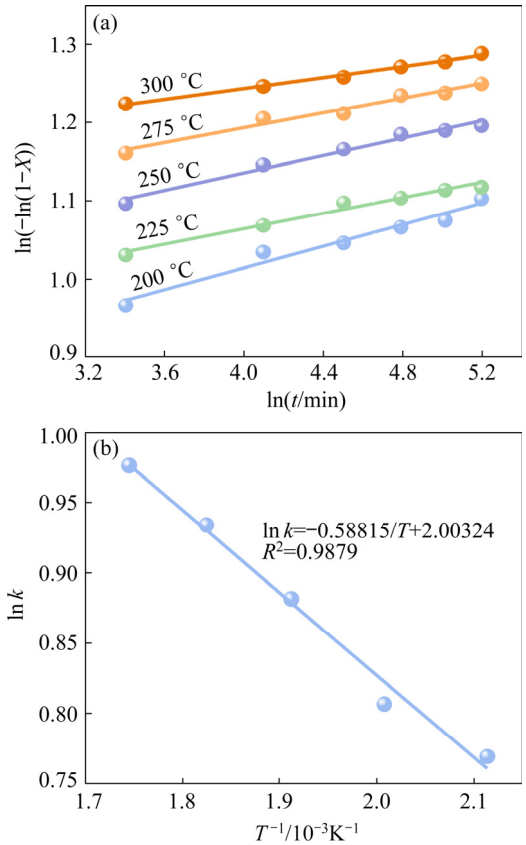

Fig. 6 Plots of $\ln(-\ln(1-X))$ vs $\ln t$ (a) and $\ln k$ vs T^{-1} (b) for roasting process

3.5 Phase transformation during roasting process

Elemental and proximate analysis of the roasted residue is shown in Table 3 and Fig. 7(a) under optimal conditions. The content of fluorine in SCC was reduced from 9.77 wt.% to 0.30 wt.%, corresponding to the fluorine removal rate of 97.82%. Furthermore, the result demonstrated that the soluble fluorine content of the roasted residue was 50.13 mg/L, which was inferior to the emission restrictions (100 mg/L) of hazardous waste recognition criterion for the Chinese National Standard (GB 5085.3—2007). And it could be observed that the fixed carbon content decreased

Table 3 Elemental analysis result of roasted residue (wt.%)

C	S	O	Na	Al	Ca
36.49	25.94	21.52	7.58	4.01	2.17
K	Fe	F	Si	Others	
0.78	0.73	0.30	0.29	0.20	

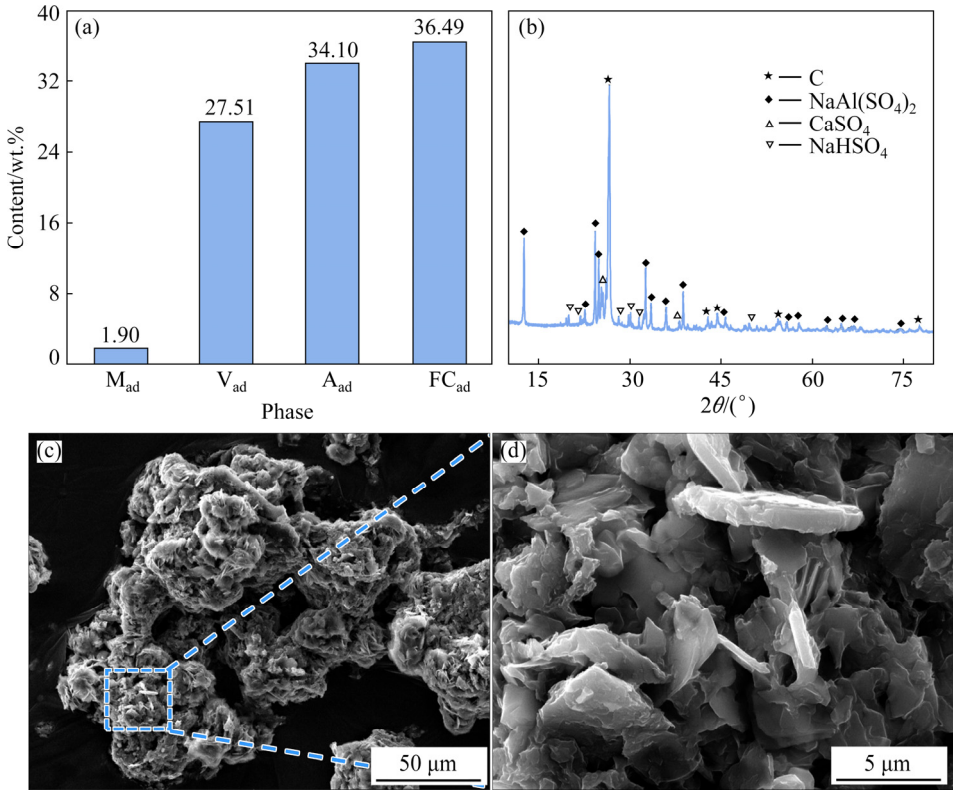

Fig. 7 Characteristics of roasted residue: (a) Proximate analysis result; (b) XRD pattern; (c, d) SEM images

and the volatile content increased compared with SCC. The conversion of fluorides and oxides to sulfates led to an increase in the total mass of roasted carbon during the roasting process, while a relative decrease in fixed carbon content.

XRD pattern was obtained and depicted in Fig. 7(b). And the main phases were C (PDF #41-1487), $CaSO_4$ (PDF #37-1496), $NaHSO_4$ (PDF #26-0960) and $NaAl(SO_4)_2$ (PDF #27-0631) in the roasted residue, while there were no characteristic peaks of fluorine-containing compounds. This indicated that fluorine was effectively removed from SCC by sulfation roasting and transformed into water-soluble sulfate, which was beneficial to further recovery of carbonaceous materials. Figures 7(c, d) manifested that many flakes agglomerated to form particles of about 100 μm. And fewer impurities were dispersed in the roasted residue.

3.6 Analysis of water-leaching process

Fluorine could be efficiently removed by the low-temperature sulfation roasting, and sulfate was formed in the process which was mixed with the carbon. To recycle the carbon materials with high purity, water leaching was carried out to eliminate the soluble sulfate (Fig. S2). And the factors were further investigated to optimize the process. The carbon content increased rapidly from 88.86 to 95.55 wt.% as the temperature increased from 20 to 40 °C (Fig. 8(a)), which was due to the higher solubility of sulfate and diffusion rate with the growing of the leaching temperature [36]. It had little effect on the improvement of carbon content when the leaching temperature exceeded 40 °C. Figure 8(b) exhibits the relationship between the carbon content and leaching time. The carbon content increased rapidly from 90.23 to 95.89 wt.% as the leaching time extended from 0.5 to 2 h. And it showed a similar trend for the influence of liquid-to-solid ratios on the carbon content (Fig. 8(c)). The carbon content in the leached residue increased significantly from 90.71 to 95.68 wt.% with the elevation of the liquid-to-solid ratio from 5:1 to 20:1. The solution reached the saturation before the soluble sulfate was completely dissolved, and the high viscosity of the leaching solution affected the mass transfer and diffusion rate when the liquid-to-solid ratio was low [37]. Therefore, the optimization of the water leaching process could be obtained by univariate experiments.

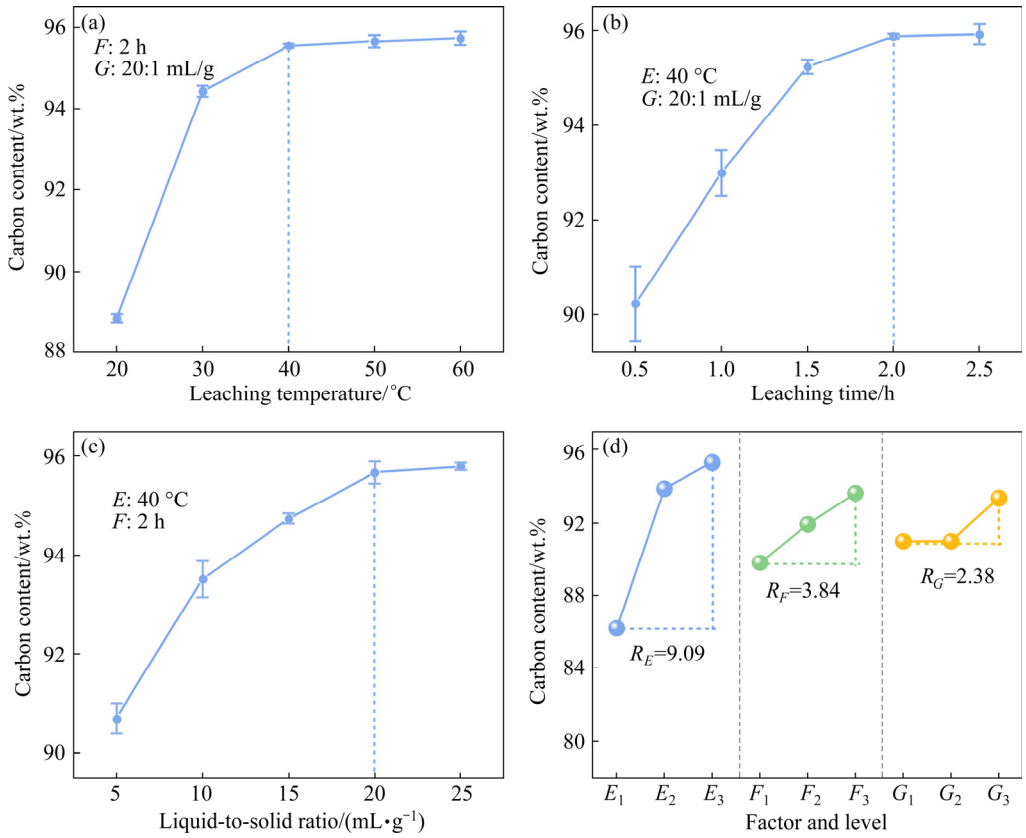

Fig. 8 Effects of parameters on carbon content: (a) Leaching temperature; (b) Leaching time; (c) Liquid-to-solid ratio; (e) K_{ij} and R_j values of different factors

Orthogonal experiments were also designed to investigate the effects of parameters on the carbon content. The factor and level are listed in Table S5 and the results of the $L_9(3^4)$ orthogonal experiments are given in Table S6. The values of extreme differences for leaching temperature (E), time (F) and liquid-to-solid ratio (G) were 9.09, 3.84 and 2.38, respectively (Fig. 8(d)). This indicated that leaching temperature had a more substantial effect on the carbon content, followed by the time and liquid-to-solid ratio. By taking the influence level of each factor, energy consumption and the amount of wastewater into consideration, the optimal condition were leaching at 40 °C for 2 h with a liquid-solid ratio of 20:1.

The roasted residue is flaky and agglomerated with each other, and the leaching process cannot be guaranteed to proceed uniformly inward from all directions, which dissatisfies the assumptions of the shrinking core model [22]. Therefore, Avrami equation was also employed to match the kinetics model for water leaching process. Figure 9(a) shows the $\ln(-\ln(1-X))$ versus $\ln t$ at different temperatures, and Table S7 lists the linear fitting results. The average of the correlation coefficient was calculated to be 0.95743 at different temperatures, suggesting that the water leaching process was matched with the Avrami model well. The Avrami exponent (n) was obtained to be 0.11675 (n<0.5), which indicated that the leaching procedure belonged to a diffusion-controlled process. It was consistent with the initial rate of reaction being fast at different temperatures. The plot of $\ln k$ versus T^{-1} is shown in Fig. 9(b). The activation energy and frequency factor of the leaching process were calculated to be 18.37 kJ/mol and 1611.74, respectively. Therefore, the water leaching process was a diffusion-controlled process, which was in agreement with the result obtained based on n<0.5. And the kinetic equation of the water leaching is

$$-\ln(1-X)=1611.74\exp[-18368/(RT)]t^{0.1167} \quad (16)$$

The leaching procedure was implemented under optimal conditions. And the elemental analysis results of the leaching residue and leachate are given in Table 4. The fixed carbon content was 90.29 wt.% in the leaching residue after deducting

volatile matter, which was increased by 27.25 wt.% compared to the SCC. And sulfur mainly existed in the leachate, which indicated that complex sulfate contaminant was withdrawn during the water leaching procedure. XRD pattern of the lixiviate dreg is depicted in Fig. 10(a). It was clearly revealed that the primary phase in the lixiviate dreg was carbon. The leachate was roasted at 300 °C and the XRD pattern of the crystalline matter is exhibited in Fig. 10(b). It could be seen that it was mainly composed of many sulfides, such as $Al_2(SO_4)_3$ (PDF #30-0043), Na_2SO_4 (PDF #37-0808), and $Fe_2(SO_4)_3$ (PDF #42-0225). Therefore, the leachate could be directly discharged without any pollution, while the recovery of valuable sulfides could be recovered. Figures 10(c, d) show the SEM images of leaching residue. It could be found that the carbon was more uniformly dispersed in the form of flakes with less impurities.

Table 4 Elemental analysis results of leaching residue and leachate (wt.%)

Sample	C	S	Ca	O	K	Na	F	Si	Al	Fe	Others
Leaching residue	90.29	1.98	1.64	1.36	1.10	0.78	0.78	0.72	0.61	0.37	0.36
Leachate	–	39.20	2.10	38.83	–	10.57	–	–	–	1.09	1.19

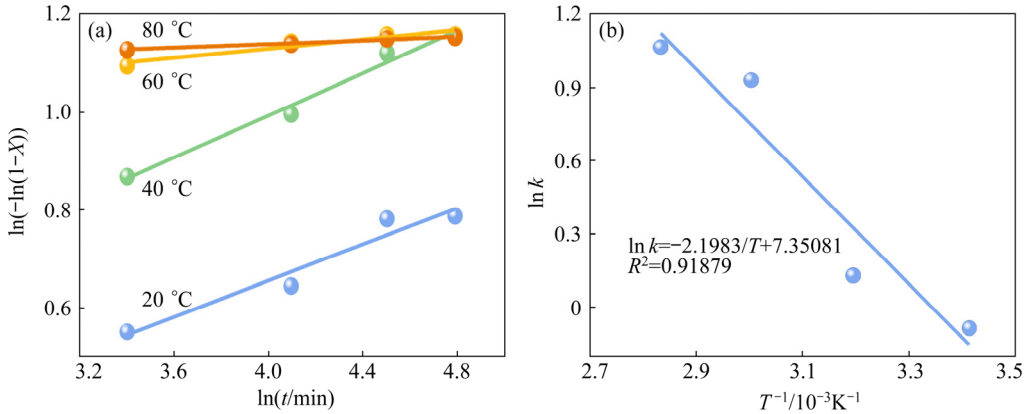

Fig. 9 Plots of ln(−ln(1−X)) vs ln t (a), and ln k vs T^{-1} (b) for water leaching process

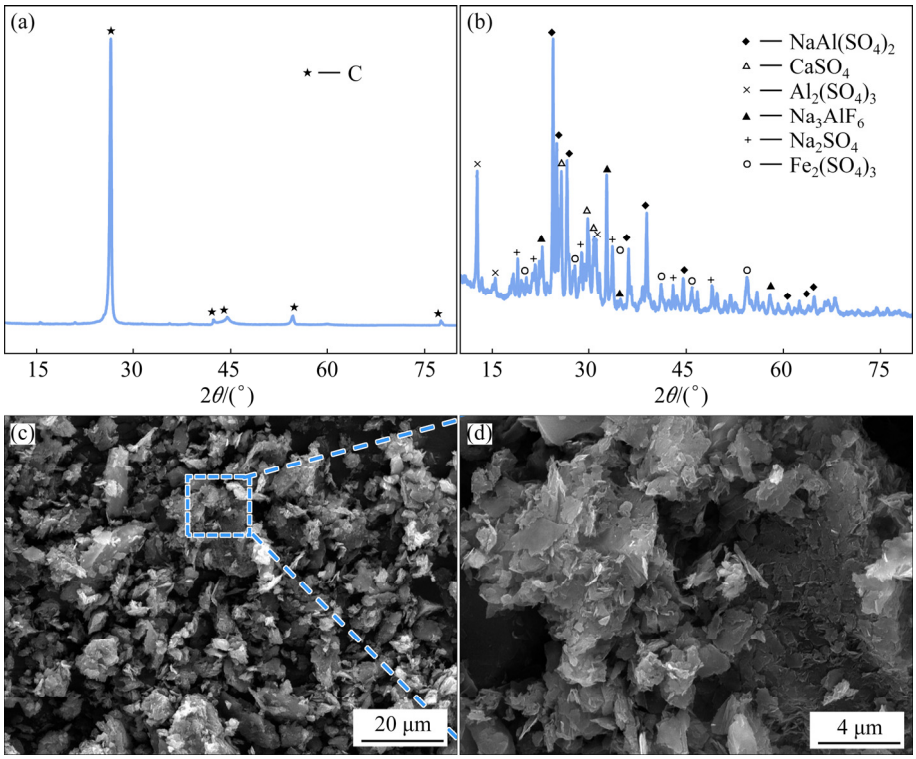

Fig. 10 XRD patterns of leaching residue (a) and leachate roasted at 300 °C (b), and SEM images of leaching residue (c, d)

4 Conclusions

(1) Thermodynamic analysis indicated that the fluorine-containing impurities could react with sulfuric acid and convert into the water-soluble sulfate at 100−300 °C. And the content of fluorine in SCC was reduced from 9.77 to 0.30 wt.%, corresponding to the fluorine removal rate of 97.82% when SCC with a grain size of <0.15 mm was mixed at a liquid-to-solid ratio of 1:1, and then roasted at 300 °C for 0.5 h. The roasting procedure was restrained by the diffusion according to the Avrami exponents n (0.05162) and the activation energy (4.89 kJ/mol).

(2) High-purity carbon (90.29 wt.%) would be obtained when roasted residue was mixed with water at a liquid-to-solid ratio of 20:1 and kept at 40 °C for 2 h, which was increased by 27.25 wt.% compared to the SCC. The Avrami exponents (n=0.11675) and activation energy (18.37 kJ/mol) also implied that the leaching procedure was also controlled by diffusion. Meanwhile, the carbon was more uniformly dispersed in the form of flakes.

Supporting Information

Supporting Information in this paper can be found at: http://www.ysxbcn.com/download/25-p3810-2022-0080-Supporting_information.pdf.

Acknowledgments

The authors are grateful for the financial support from the Natural Science Foundation of Hunan Province, China (No. 2020JJ1007).

References

[1] YANG Yi, GUO Yao-qi, ZHU Wen-song, HUANG Jian-bai. Environmental impact assessment of China's primary aluminum based on life cycle assessment [J]. Transactions of Nonferrous Metals Society of China, 2019, 29(8): 1784−1792.

[2] SENANU S, WANG Zhao-hui, RATVIK A P, GRANDE T. Carbon cathode wear in aluminium electrolysis cells [J]. JOM, 2020, 72(1): 210−217.

[3] TROPENAUER B, KLINAR D, SAMEC N, GOLOB J, KORTNIK J. Sustainable waste-treatment procedure for the spent potlining (SPL) from aluminium production [J]. Materiali in Tehnologije, 2019, 53(2): 277−284.

[4] XIE Ming-zhuang, LI Rong-bin, ZHAO Hong-liang, LIU Wei, LU Ting-ting, LIU Feng-qin. Detoxification of spent cathode carbon blocks from aluminum smelters by joint controlling temperature-vacuum process [J]. Journal of Cleaner Production, 2020, 249: 119370.

[5] CHEN Zi-hong, LIU Jing-yong, CHEN Lai-guo, EVRENDILEK F, XIE Wu-ming, WU Xie-yuan, HU Jin-wen, LI Wei-xin. Emission-to-ash detoxification mechanisms of co-combustion of spent pot lining and pulverized coal [J]. Journal of Hazardous Materials, 2021, 418(18): 126380.

[6] LIU Feng-qin, LV Han, ZUO Zheng-ping, XIE Ming-zhuang, LI Rong-bin, ZHAO Hongliang. A denitrification-phase transition and protection rings (DPP) process for recycling electrolytic aluminum dross [J]. ACS Sustainable Chemistry & Engineering, 2021, 9(41): 13751−13760.

[7] YANG Kai, GONG Pei-yu, TIAN Zhong-liang, LAI Yan-qing, LI Jie. Recycling spent carbon cathode by a roasting method and its application in Li-ion batteries anodes [J]. Journal of Cleaner Production, 2020, 261: 121090.

[8] LIU Feng-qin, XIE Ming-zhuang, LIU Wei, ZHAO Hong-liang. Footprint of harmful substances in spent pot lining of aluminum reduction cell [J]. Transactions of Nonferrous Metals Society of China, 2020, 30(7): 1956−1963.

[9] LI Xiao-ming, YIN Wei-dong, FANG Zhao, LIU Qi-hang, CUI Ya-ru, ZHAO Jun-xue, JIA Hao. Recovery of carbon and valuable components from spent pot lining by leaching with acidic aluminum anodizing wastewaters [J]. Metallurgical and Materials Transactions B: Process Metallurgy and Materials Processing Science, 2019, 50(2): 914−923.

[10] HOLYWELL G, BREAULT R. An overview of useful methods to treat, recover, or recycle spent potlining [J]. JOM: The Journal of the Minerals, Metals & Materials Society, 2013, 65(11): 1441−1451.

[11] YAO Zhen, ZHONG Qi-fan, XIAO Jin, YE Sheng-chao, TANG Lei, ZHANG Zhenhua. An environmental-friendly process for dissociating toxic substances and recovering valuable components from spent carbon cathode [J]. Journal of Hazardous Materials, 2021, 404: 124120.

[12] XIE Ming-zhuang, ZHAO Hong-liang, WU Ze-gang, LIU Wei, LI Rong-bin, LIU Feng-qin. Study on kinetics of vacuum heat treatment process of the spent cathode carbon blocks from aluminum smelters [J]. Journal of Sustainable Metallurgy, 2020, 6(4): 715−723.

[13] LI Nan, XIE Gang, WANG Zu-xu, HOU Yan-qing, LI Rong-xing. Recycle of spent potlining with low carbon grade by floatation [J]. Advanced Materials Research, 2014, 881/882/883: 1660−1664.

[14] LI Nan, JIANG Yan, LV Xiang, GAO Lei, CHATTOPADHYAY K. Vacuum distillation-treated spent potlining as an alternative fuel for metallurgical furnaces [J]. JOM, 2019, 71(9): 2978−2985.

[15] SAJWANI A. The application of the environmental management system at the aluminum industry in UAE [J]. International Journal of Geomate, 2017, 12(30): 1−10.

[16] SHI Zhong-ning, LI Wei, HU Xian-wei, REN Bi-jun, GAO Bing-liang, WANG Zhao-wen. Recovery of carbon and cryolite from spent pot lining of aluminium reduction cells by chemical leaching [J]. Transactions of Nonferrous Metals Society of China, 2012, 22(1): 222−227.

[17] NIE Yun-fei, GUO Xin-yao, GUO Zhao-hui, TANG Jian-guo, XIAO Xi-yuan, XIN Li-qing. Defluorination of spent pot lining from aluminum electrolysis using acidic iron-containing solution [J]. Hydrometallurgy, 2020, 194: 105319.

[18] YUAN Jie, XIAO Jin, TIAN Zhong-liang, YANG Kai, YAO Zhen. Optimization of spent cathode carbon purification process under ultrasonic action using taguchi method [J]. Industrial & Engineering Chemistry Research, 2018, 57(22): 7700−7710.
[19] KRYSENKO G F, GORDIENKO P S, EPOV D G. Sulfuric acid breakdown of fluorite in the presence of silica [J]. Russian Journal of Inorganic Chemistry, 2009, 54(12): 1876−1879.
[20] PAULINO J F, NEUMANN R, AFONSO J C. Evaluation of cryolite from pitinga (Amazonas-Brazil) as a source of hydrogen fluoride [J]. Química nova, 2016, 39(4): 496−501.
[21] DYACHENKO A N, KRAYDENKO R I, LESNIKOVA M S, MALYUTIN L N, PETLIN I V. Physics and chemistry of the hydrogen fluoride production process from fluorine containing waste [J]. IOP Conference Series: Materials Science and Engineering, 2016, 135(1): 12012.
[22] DYACHENKO A N, PETLIN I V, MALYUTIN L N. The research of sulfuric acidic recycling of aluminum industry fluorine-containing waste products [J]. Procedia Chemistry, 2014, 11: 10−14.
[23] MATHIESSEN B, JENSEN M, ZHURAVLEV F. [18F]Fluoride recovery via gaseous [18F]HF [J]. Journal of Labelled Compounds & Radiopharmaceuticals, 2011, 54(13): 816−818.
[24] QU Xin, XIE Hong-wei, CHEN Xiang, TANG Yi-qi, ZHANG Bei-lei, XING Peng-fei, YIN Hua-yi. Recovery of $LiCoO_2$ from spent lithium-ion batteries through a low-temperature ammonium chloride roasting approach: Thermodynamics and reaction mechanisms [J]. ACS Sustainable Chemistry & Engineering, 2020, 8(16): 6524−6532.
[25] LISBONA D F, SOMERFIELD C, STEEL K M. Leaching of spent pot-lining with aluminium nitrate and nitric acid: Effect of reaction conditions and thermodynamic modelling of solution speciation [J]. Hydrometallurgy, 2013, 134/135(3): 132−143.
[26] XIAO Jin, YUAN Jie, TIAN Zhong-liang, YANG Kai, YAO Zhen, YU Bai-lei, ZHANG Liu-yun. Comparison of ultrasound-assisted and traditional caustic leaching of spent cathode carbon (SCC) from aluminum electrolysis [J]. Ultrasonics Sonochemistry, 2018, 40: 21−29.
[27] WANG Ming-yu, XIAN Peng-fei, WANG Xue-wen, LI Bo-wen. Extraction of vanadium from stone coal by microwave assisted sulfation roasting [J]. JOM, 2015, 67(2): 369−374.
[28] CHANG Jun, ZHANG Li-bo, YANG Chang-jiang, YE Qain-xu, CHEN Jing, PENG Jin-hui, SRINIVASAKANNAN C, LI Wei. Kinetics of microwave roasting of zinc slag oxidation dust with concentrated sulfuric acid and water leaching [J]. Chemical Engineering and Processing: Process Intensification, 2015, 97: 75−83.
[29] CUI Chuan-wen, SHI Feng, LI Yu-guo, WANG Shu-yun. Orthogonal analysis for perovskite structure microwave dielectric ceramic thin films fabricated by the RF magnetron-sputtering method [J]. Journal of Materials Science: Materials in Electronics, 2009, 21(4): 349−354.
[30] ZHENG Ya-jie, CHEN Kun-kun. Leaching kinetics of selenium from selenium-tellurium-rich materials in sodium sulfite solutions [J]. Transactions of Nonferrous Metals Society of China, 2014, 24(2): 536−543.
[31] ILHAN S, AKGÜN D. Leaching kinetics of Mo, Ni, and Al oxides from spent nickel-molybdenum hydrodesulfurization catalyst in H_2SO_4 solution [J]. Journal of Sustainable Metallurgy, 2021, 7(2): 470−480.
[32] ZHANG Jia-liang, HU Jun-tao, ZHANG Wen-juan, CHEN Yong-qiang, WANG Cheng-yan. Efficient and economical recovery of lithium, cobalt, nickel, manganese from cathode scrap of spent lithium-ion batteries [J]. Journal of Cleaner Production, 2018, 204: 437−446.
[33] TIAN Jia, ZHANG Xing-fei, WANG Yu-feng, HAN Hai-sheng, SUN Wei, YUE Tong, SUN Jing-tao. Alkali circulating leaching of arsenic from copper smelter dust based on arsenic-alkali efficient separation [J]. Journal of Environmental Management, 2021, 287: 112348.
[34] LOGAN S R. The origin and status of the Arrhenius equation [J]. Journal of Chemical Education, 1982, 59(4): 279−281.
[35] SANTOS F M F, PINA P S, PORCARO R, OLIVEIRA V A, SILVA C A, LEAO V A. The kinetics of zinc silicate leaching in sodium hydroxide [J]. Hydrometallurgy, 2010, 102(1): 43−49.
[36] YOU Zhi-xiong, LI Guang-hui, ZHANG Yuan-bo, PENG Zhi-wei, JIANG Tao. Extraction of manganese from iron rich MnO_2 ores via selective sulfation roasting with SO_2 followed by water leaching [J]. Hydrometallurgy, 2015, 156: 225−231.
[37] ZHANG Ya-li, YU Xian-jin, LI Xiao-bin. Zinc recovery from franklinite by sulphation roasting [J]. Hydrometallurgy, 2011, 109(3): 211−214.

一种实现废阴极炭回收以及高效脱氟的环保可持续工艺

李怡凡[1]，程 皓[1]，龚培育[1]，杨 凯[2]，田忠良[1]，赖延清[1]

1. 中南大学 冶金与环境学院，长沙 410083；2. 西安建筑科技大学 冶金工程学院，西安 710055

摘 要：提出一种系统、绿色的低温硫酸化焙烧−水浸工艺，危险固体废弃物废阴极炭块的脱氟率可达 97.82%，同时，片状回收炭纯度达 90.29%(质量分数)。热力学分析和 SEM、XRD 及 EDS 结果表明，大部分的氟化物可以在较低的温度下转化为水溶性的硫酸盐。结果表明，将<0.15 mm 的废阴极颗粒与浓硫酸以 1:1 的液固比混合，然后在 300 °C 焙烧 0.5 h 可实现最佳的脱氟效果。进一步通过水浸去除硫酸盐实现炭的纯化。同时，焙烧和浸出过程的 Avrami 指数和相应的活化能表明这两个过程均受扩散控制。

关键词：废阴极；脱氟；硫酸化焙烧；水浸；动力学分析

(Edited by Bing YANG)